Preprints of the 2012 20th Mediterranean Conference on Control & Automation (MED), Barcelona, Spain, July 3-6, 2012

Dynamic Positioning of a Marine Vessel using DTVSC and Robust Control Allocation

Flavia Benetazzo, Gianluca Ippoliti, Sauro Longhi, Paolo Raspa and Asgeir J. Sørensen

Abstract— **This paper presents a discrete-time variable-structure control (DTVSC) for the dynamic positioning system of a marine vessel. The DTVSC guarantees robustness with respect to environmental disturbances. Moreover, the allocation problem, in the case of vessels with azimuth thrusters, represents a challenging problem since a non-convex nonlinear problem must be solved. In this paper, the allocation problem is solved using the Damped Least Squares method. The proposed solution is compared with a PID-based control. Reported simulations show that the proposed solution produces better performance.**

I. INTRODUCTION

The Dynamic Positioning is a controlled system aimed to automatically maintain the vessel position and heading (on a fixed location or with a pre-determined track) by means of its propulsion and manoeuvring thrusters. Knowledge of thruster allocation, combined with information from the sensors (GPS, gyroscopes, etc), can be used to calculate the steering angle and the thrust for each thruster. This allows to automatically maintain the desired position and orientation according to a navigation path or a specific task (absolute or relative DP).The Dynamic Positioning System can be decisive in case where the position of the unit is bound to a specific point on the seabed (absolute DP). Or the desired position is relative to a moving unit. An example is a ship involved in operations with other vessels and remotely operated or autonomous underwater vehicles for hydrocarbon exploration.

A survey of dynamic positioning control systems in the last decades is available from [1]. The first DP systems were designed using conventional PID controllers in cascade with low pass and/or notch filters to suppress the wave induced motion components. From 1980 a new model-based control concept, that uses stochastic optimal control theory, was employed with the DP problem by [2]. Later extensions and modifications of this work have been proposed by numerous other authors, like [3], [4] and [5].

In order to control the motion of a ship with respect to surge, sway and yaw, a minimum set of thrust devices is required. For a given control command there exist several thrust combinations that satisfy the control command. The solution of the thrust allocation problem determines how much thrust should be provided by each of the thrust devices when a given force/moment command is issued by a higher-level controller. Previous works on thrust allocation have been presented by [6], [7] and [8], proposed to split the allocation problem into two subproblems: static and dynamic. The static solution is obtained using the *Damped Least Squares* method, that guarantees the existence of the solution also in case of singularities. The dynamic solution is obtained assuming that the thrust command can be perturbed about the static solution. In [9] both implicit and explicit methods formulated as optimization problems are discussed.

In this paper an innovative solution for the DP control system is proposed, based on the robust Discrete-Time Variable Structure Controller (DTVSC) along with a robust thuster allocator. The introduction of DTVSC, allows to take directly into account the issue of control law digitalization and to ensure robustness with respect to model uncertainties and input disturbances acting on the actuators.

The paper is organized as follows. The kinematic and dynamic equations, the thruster allocation, the wave model and the measurement system are presented in Section II. The control system, in particular the DTVS controller, is reported in Section III. The allocation problem is discussed in Section IV. The model and the simulation results are presented in Section V. The paper ends with conclusions and comments.

II. SHIP MODEL

In this section, the process plant model including the kinematics and dynamics will be discussed along with the reference frames and environmental disturbances.

A. Reference frames

The ship motion can be represented relative to different reference frames, three different reference frames are considered in this paper, the $\{n\}$ (North-East-Down) frame, which has a fixed origin relative to the earth (earth fixed) at the mean water level, the $\{d\}$ reference-parallel frame and the $\{b\}$ frame, fixed at the center of gravity (CG) of the vessel. North-East-Down, reference-parallel and body-fixed frames are shown in Fig. 1. The generalized displacement and body-fixed velocities are defined as η and ν respectively. Where ν is defined in the $\{b\}$ frame, while η is defined in the $\{n\}$ frame.

$$\begin{aligned} \eta &= [n, e, d, \phi, \theta, \psi]^T \\ \nu &= [u, v, w, p, q, r]^T \end{aligned} \tag{1}$$

F. Benetazzo, G. Ippoliti, S. Longhi and P. Raspa are with the Dipartimento dell'Ingegneria dell'Informazione, Universit Politecnica delle Marche, Via brecce Bianche, 60131 Ancona AN, Italy {f.benetazzo, gianluca.ippoliti, sauro.longhi, p.raspa}@univpm.it

A. J. Sørensen is with the Department of Marine Technology, the Norwegian University of Science and Technology (NTNU), NO-7941 Throndeim, Norway asgeir.sorensen@ntnu.no

978-1-4673-2529-5/12/$31.00 ©2012 IEEE

B. Kinematics and dynamics equations

The dynamics of marine vessels can be divided in two parts, the kinematics and the dynamics. The latter analyses the forces causing the ship motion, while the former accounts only for the geometric aspects of the motion. The kinematics equations, which express the relationship between the generalized displacements in the $\{n\}$ frame and the velocities in the $\{b\}$ frame, are:

$$\dot{\eta} = J(\eta)\nu \tag{2}$$

From [10], in case of irrotational and constant ocean currents, the 6 degrees of freedom (DOF) maneuvering equations of motions can be expressed in the $\{b\}$ frame by

$$M\dot{\nu}_r + C(\nu_r)\nu_r + D(\nu_r)\nu_r + G\eta = \tau_c + \tau_{env} \tag{3}$$

where $\nu_r = [u - u_c, v - v_c, w, p, q, r]^T$ is the relative velocity vector between the vessel and current, as explained in Section II-C.3; $M = (M_{RB} + M_A)$ is the system inertia matrix, including the rigid-body and the added mass matrices; $C = C_{RB} + C_A(\nu)$ is the Coriolis-centripetal matrix, including both rigid-body and added mass; $D(\nu_r) = D_L + D_{NL}(\nu_r, \gamma_r)$ is the damping matrix, which may be divided into a linear component, D_L, accounting for linear wave drift damping and laminar skin frictions and a non linear component $D_{NL}(\nu_r, \gamma_r)$ accounting for the effects of ocean currents. It is important to notice that, for velocities of vessel close to zero, the linear damping becomes more significant than the nonlinear damping. The restoring term is assumed to be $G(\eta) = G\eta$ under the assumption of small roll and pitch angles. The τ_c are the control forces and moments to be produced by the actuators, while τ_{env} are the environmental loads.

C. Environmental Forces and moments

A ship in a seaway is mainly affected by the following types of environmental disturbances: waves, currents, wind. The environmental disturbances contain both slowly varying and high-frequency forces. Control forces and moments due to environmental disturbances are coursed by wind and waves. Using the principle of superposition, they are added to the right side of (3) by defining: $\tau_{env} = \tau_{wind} + \tau_{wave}$.

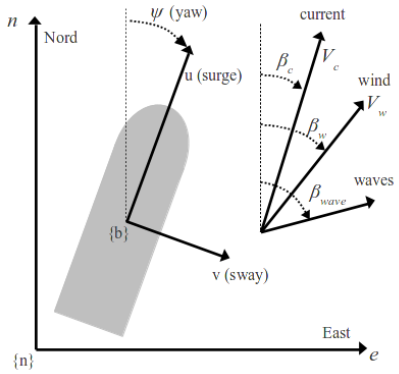

Fig. 1. Reference frames definition: $\{n\}$ and $\{b\}$ frames, waves, current and wind directions

1) Wind forces and moments: The wind force on a marine vessel is proportional to the projected area above the waterline and to the square of the wind speed relative to the vessel. The total relative wind speed can be defined as:

$$U_{rw} = \sqrt{u_{rw}^2 + v_{rw}^2} \tag{4}$$

where $u_w = u - V_w \cos(\gamma_{rw})$ and $v_w = v - V_w \sin(\gamma_{rw})$ are the wind speeds components, V_w is the wind velocity, $\gamma_{rw} = \beta_w - \psi$ is the relative wind angle and β_w is the wind direction. The parameters above are expressed in the $\{n\}$ frame (see Fig. 1). Then the wind loads are given by [10]

$$\tau_{wind} = \frac{1}{2}\rho_a U_{rw}|U_{rw}|C_w(\gamma_w)A_{xyz}L_{xy} \tag{5}$$

where ρ_a is the air density; A_{xyz} is a matrix whose coefficients are the lateral (A_x) and longitudinal (A_y) areas of the non-submerged part of the ship projected on the xz- and yz-plane; L_{xy} is a matrix whose coefficients are overall length of vessel (L_{oa}) and vertical distances between transverse and longitudinal origin and the wind load point of attack, (L_{xy} and L_{yz}); $C_w(\gamma_w)$ are the non-dimensional wind coefficients. These coefficients are often derived by model testing or by semi-empirical formulas, as in [11].

2) Wave forces and moments: When designing a DP control system it is important to evaluate the robustness and performance in the presence of waves. A motion control system can be simulated under influence of wave-induced forces by separating two effects: the 1-st order wave-induced forces, τ_{wave1}, wave loads observed as zero-mean oscillatory components and the 2-nd order wave-induced forces, τ_{wave2}, wave drifts forces observed as non-zero slowly varying components. According to [10] wave forces can be modelled by a linear superposition of the two components, therefore $\tau_{wave} = \tau_{wave1} + \tau_{wave2}$.

Wave force models depends on response amplitude operators (RAOs) computed for the particular craft using a hydrodynamic program from hull geometry. For each degree of freedom (dof $\in \{1...6\}$) in (1), the wave loads and drifts can be represented as a sum of a large number N of sinusoidal components:

$$\begin{aligned}
\tau_{wave1}^{\{\text{dof}\}} &= \sum_{k=1}^{N} \rho_{\text{w}} g \left|F_{wave1}^{\{dof\}}\right| A_k \cos\left(\omega_{e_k} t + \angle F_{wave1}^{\{dof\}} + \epsilon_k\right) \\
\tau_{wave2}^{\{\text{dof}\}} &= \sum_{k=1}^{N} \rho_{\text{w}} g \left|F_{wave2}^{\{dof\}}\right| A_k^2 \cos\left(\omega_{e_k} t + \epsilon_k\right)
\end{aligned} \tag{6}$$

Where the normalised force RAO $F_{wavei}^{\{\text{dof}\}} = F_{wavei}^{\{\text{dof}\}}(\omega_k, \beta_{wave})$ are complex variables depending on the wave frequency component ω_k and the relative wave direction β_{wave}, ρ_{w} is the water density, A_k is the wave amplitude for the wave component k, depending on the wave spectrum, significant wave height H_s and modal frequency w_0. The wave encounter frequency is $\omega_{e_k} = \omega_k - \left(\omega_k^2 U \cos(\beta_{wave})\right)/(2g)$, U is the ship forward velocity and ϵ_k is a random phase component drawn from

an uniform distribution in $[-\pi\ \pi]$, to ensure stationarity of the time series.

By lack of space, this paper does not focus on the wave filtering problem. For reference a common approach based on the Extended Kalman Filter has been used, see [16] for more details and comparisons of the current approach with other standard methods.

3) Ocean current forces and moments: The effect of sea current can be divided into 2 components: potential and viscous. The potential component of current includes the so called Munk moment and is formulated according to [12] as $C_A(\nu_r)$ in (3).

The horizontal current components in surge and sway are defined as:

$$u_c = V_c \cos(\beta_c - \psi) \qquad v_c = V_c \sin(\beta_c - \psi), \tag{7}$$

where V_c and β_c are the current velocity and direction respectively, see Fig. 1. The total relative current vector is then defined as:

$$U_{cr} = \sqrt{u_r^2 + v_r^2}, \tag{8}$$

where $u_r = u - u_c$, and $v_r = v - v_c$. The effect of the current are normally included in the nonlinear damping term $D_{NL}(\nu_r, \gamma_r)$ of (3) as a function of the relative velocity vector ν_r and the relative drag angle, $\gamma_r = \arctan(-v_r, u_r)$.

III. CONTROL SYSTEM

A robust non-linear design technique for marine craft is the Variable Structure Control (VSC) with sliding modes, which is described in [13], [14]. The Variable Structure Control is a state-feedback technique, which allows to handle model uncertainties. Each state component can be equal to one of two state functions: the switching determines the discontinuity. The control objective is to force the state to reach the intersection of switching surface and stay inside it. Designing the Variable Structure Control law in digital form ensures robustness with respect to model uncertainties and input disturbances acting on the actuators. Applications of DTVSC are listed in [15], [16], and [17]. In this section the introduction of a VSC control system for Dynamic Positioning based on the Discrete-Time Variable Structure Controller using two-steps sliding surfaces is reported. The slow manoeuvring model of a vessel in a seaway can be obtained to model the response of the vessel to the control action, writing (3) and (2) as follows:

$$\begin{aligned} \dot{\nu}_r &= -M^{-1}\left(C(\nu_r) + D(\nu_r)\right)\nu_r - M^{-1}G\eta + M^{-1}\tau_c \\ \dot{\eta} &= J(\eta)\nu \end{aligned} \tag{9}$$

The discretization of the (9) with a sampling time T_c using common techniques , see [18], gives:

$$\begin{aligned} \nu_r(k+1) &= \Phi_\nu \nu_r(k) + \Phi_\eta \eta(k) + \Gamma\tau_c(k) \\ &\text{with} \\ \Phi_\nu &= \exp^{-\left(M^{-1}(C(\nu_r(k)) + D(\nu_r(k)))\right)T_c} \\ \Phi_\eta &= \exp^{-M^{-1}GT_c} \\ \Gamma &= M^{-1}T_c \end{aligned} \tag{10}$$

We define the generalised velocity vector in body-fixed frame to be imposed by the control law as $\tau_d(k) = \Gamma\tau_c(k)$. Hence, the following discrete dynamic model is obtained:

$$\nu_r(k+1) = \Phi_\nu \nu_r(k) + \Phi_\eta \eta(k) + \tau_d(k) \tag{11}$$

Under the assumption of DP control, only 3 DOF, namely surge, sway and yaw, are actively controlled,hence $\tau_d = \left[\tau_d^1, \tau_d^2, 0, 0, 0, \tau_d^6\right]^T$. To account for possible model uncertainties, it is assumed that the model parameters may differ from their nominal values for some unknown but bounded quantities:

$$\Phi_\nu = \overline{\Phi}_\nu + \Delta\Phi_\nu,\ \Phi_\eta = \overline{\Phi}_\eta + \Delta\Phi_\eta,\ \Gamma = \overline{\Gamma} + \Delta\Gamma \tag{12}$$

Defining the reference vessel speed in $\{b\}$ frame as $\nu_d(k)$, obtained using the inverse kinematic equation (2) and a reference path η_d in $\{n\}$ frame, the reference velocity error can be defined as:

$$\Delta\nu(k) = \nu(k) - \nu_d(k) \tag{13}$$

Using (13) we can define the two-steps sliding surfaces as:

$$s(k) = \Delta\nu(k) + \lambda_1\Delta\nu(k-1) + \lambda_2\Delta\nu(k-2) = 0 \tag{14}$$

where λ_1, λ_2 are parameters to choose in order to ensure that the zeros of (14) are inside the unit circle. The condition $\lim_{k\to\infty} s(k) = 0$ must be met to reach the control objective. In order to satisfy this specification, the following condition must be verified:

$$|s(k+1)| < |s(k)| \tag{15}$$

From (15), defining $\Delta s(k+1) = s(k+1) - s(k)$, the discrete sliding mode existence condition is obtained:

$$s(k)^T\Delta s(k+1) < -\frac{1}{2}(\Delta s(k+1))^T(\Delta s(k+1)) \tag{16}$$

Let us consider the following control law

$$\tau_d(k) = \tau_d^{eq}(k) + \tau_d^{nom}(k) \tag{17}$$

where, using (11), (12) and (14), we define

$$\begin{aligned} \tau_d^{eq}(k) &= \nu(k) - \overline{\Phi}_\nu\nu(k) - \overline{\Phi}_\eta\eta(k) - s(k) \\ \tau_d^{nom}(k) &= \begin{cases} \vartheta(|s(k)| - \rho) & if \quad |s(k)| > \rho \\ -s(k) + \tau_n^*(k-1) & if \quad |s(k)| \le \rho \end{cases} \end{aligned} \tag{18}$$

with $|\vartheta| \le 1$ and

$$\begin{aligned} \rho =& \Delta\Phi_\nu\nu_{max} + \Delta\Phi_\eta\eta_{max} + \rho^* \\ \rho^* \ge& |\ \nu^*(k+1) - \nu^*(k)| \end{aligned} \tag{19}$$

Using [15], it can be demonstrated that (17) guarantees to satisfy the condition in (16) outside a given sector defined by $|s(k)| > \rho$, where ρ, defined in (19), is the vector of maximum uncertainties of the system, which greatly depend on the area of operation of the vessel. Capability polar plots for DP, see [19], can also be considered to ease the setup of parameters in (19). Inside the sector defined by (19) the sliding condition (16) can be imposed only approximately, using the approach of *Time Delay Control*. In order to obtain

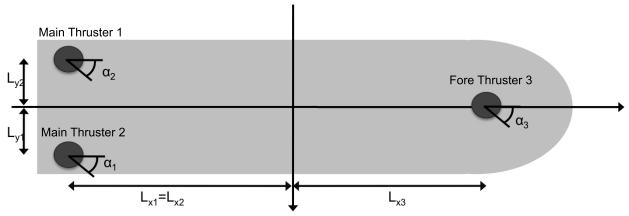

Fig. 2. Thrusters configuration for the vessel

zero steady-state errors in surge, sway and yaw directions, an integral control action τ_I can be added to the DTVS control law, see [10]. Finally the control input to the thrusters is

$$\tau_c = \Gamma^{-1}\left(\tau_d(k) + \tau_I(k)\right) \tag{20}$$

IV. CONTROL ALLOCATION

In this section the focus is on the thrust allocation problem, that is: how much thrust should be provided by each of the thrust devices. Thruster configuration is shown in Fig. 2

The aim of the control allocation is to compute azimuth thruster angle α_c and torque f_c commands in order to satisfy the control law in (20) for all thrust devices. The allocation problem can be formulated as the calculation of a pair (α_c, f_c) that satisfies:

$$\tau_c = T(\alpha_c) f_c \tag{21}$$

where $\tau_c = \tau$ is given by the control law in (20) and $T(\alpha_c)$, considering a vessel with *n* azimuth rotatable thrusters, can be written as

$$T(\alpha) = AB(\alpha) \tag{22}$$

So, equation (21) becomes:

$$\tau = T(\alpha) f = \underbrace{AB(\alpha)}_{t} f \tag{23}$$

where A is a $3 \times 2n$ matrix:

$$A = \begin{bmatrix} 1 & 0 & .. & 1 & 0 \\ 0 & 1 & .. & 0 & 1 \\ -l_{y1} & l_{x1} & .. & -l_{yn} & l_{xn} \end{bmatrix} \tag{24}$$

and B is a $2n \times n$ matrix

$$B = \begin{bmatrix} \cos(\alpha_1) & 0 & .. & 0 \\ \sin(\alpha_1) & 0 & .. & 0 \\ .. & .. & .. & .. \\ 0 & 0 & .. & \cos(\alpha_n) \\ 0 & 0 & .. & \sin(\alpha_n) \end{bmatrix} \tag{25}$$

For azimuth *i*, the angle α_i is given by:

$$\alpha_i = \arctan(t_i^y / t_i^x) \tag{26}$$

The static solution is obtained using the *Damped least squares (DLS)* method, that allows to obtain the thrust command also near a singular point. The dynamic problem is solved by assuming that the thrust command can be perturbed about the static thrust command. More information are provided in [8]. The allocation problem is divided into a static and dynamic allocation problem, to take into account the thruster dynamics. The thruster is modelled as a Low-Pass (LP) filter in static conditions. For small command deviations, it is modelled as a High-Pass (HP) filter.

A. Static Allocation

The LP-filtered command $\overline{\tau}$ is given by

$$\dot{\overline{\tau}} + \Lambda\overline{\tau} = \Lambda\tau_c \tag{27}$$

where $\Lambda = diag(\frac{1}{T_1}, \frac{1}{T_2}, \frac{1}{T_3})$ is a diagonal matrix containing time constant for surge, sway and yaw.

The LP-filtered aximuth angles and thrust forces are

$$\begin{aligned} \overline{\alpha}_i &= \arctan\left(\overline{t}_i^y / \overline{t}_i^x\right) \\ \overline{f} &= B^{\dagger}(\overline{\alpha})\overline{t} = B^T(\overline{\alpha})\overline{t} \end{aligned} \tag{28}$$

B. Dynamic Allocation

Let assume small deviations in thrust command $\Delta\tau$ around the LP-filtered thrust command $\overline{\tau}$. The change in the azimuth angles $\Delta\alpha$ and thrust forces Δf can be computed assuming a perturbation $(\Delta\alpha, \Delta f)$ about the point $(\overline{\alpha}, \overline{f})$:

$$\Delta\tau = J(\overline{\alpha}, \overline{f}) \begin{bmatrix} \Delta\alpha & \Delta f \end{bmatrix}^T \tag{29}$$

where $J\left(\overline{\alpha}, \overline{f}\right)$ is the Jacobian matrix defined as

$$J(\overline{\alpha}, \overline{f}) = \left[\frac{\partial T(\alpha) f}{\partial \alpha} T(\alpha)\right]\Bigg|_{\alpha=\overline{\alpha}\, f=\overline{f}} \tag{30}$$

The dynamic thrust command $\Delta\tau$ is computed by using a limited HP-filter of the thrust command τ_c. The filter has the form of the following transfer function:

$$\Delta\tau_i(s) = \frac{K_i s}{s^2 + s\zeta_i\omega_{n,i}s + \omega_{n,i}^2} \tau_{c,i}(s) \tag{31}$$

where $\omega_{n,i}$ is the cut-off frequency and ζ_i is the relative damping ratio in surge, sway and yaw respectively.

C. DLS Algorithm

The control allocation problem is solved superimposing the static and the dynamic solutions. Thruster angle is given by

$$\alpha_c = \overline{\alpha} + \Delta\alpha \tag{32}$$

The DLS method provides the thruster torques

$$f_c = T_{DLS}^{\dagger}(\alpha_c)\tau_c \tag{33}$$

where $T_{DLS}^{\dagger}(\alpha_c)$ is the pseudo-inverse matrix based on the *DLS*, see [8].

TABLE I

DESIRED POSITIONS

Case	Time (s)	x_d (m)	y_d (m)	ψ_d (deg)
1	0-1000	0	0	0
1	1000-2000	10	10	20
2	0-1000	0	0	0
2	1000-2000	10	10	20
3	0-800	5	3	$\arctan(y_d/x_d)$
3	800-1400s	6	3	$\arctan(y_d/x_d)$
3	1400-2000	6	7	$\arctan(y_d/x_d)$

TABLE II

ENVIRONMENTAL CONDITIONS

Case	H_s (m)	ω_0 (rad/s)	V_w (m/s)	V_c (m/s)
1	0.1	1.1109	1.5	0.05
2	0.3	1.0003	3	0.1
3	0.1	1.1109	1.5	0.05

V. RESULTS

The 1:30 scale model of a naval surveillance vessel,the *CyberShip 3* (CS3), was used for testing. This ship is located at the *Marine Cybernetics Laboratory* (MCLab), Norwegian University of Science and Technology. For more details about the CS3, see [20] and [21]. The ship is equipped with three azimuthal thrusters, as shown in Fig. 2. Hence we have 6 control variables for 3 DOF, $u = [u_1, u_2, u_3]^T$ and $\alpha = [\alpha_1, \alpha_2, \alpha_3]^T$. Here we assume state feedback, an extension to output feedback using state observers will be a next step. Thrusters positions are $L_{y1} = 0.11m$, $L_{y2} = 0.11m$, $L_{x1} = L_{x2} = 0.789m$ and $L_{x3} = 0.636m$. Referring to Fig. 2, the maximum thrust of the main thrusters is 21.9 N and the maximum thrust of the fore thruster is 10 N.

The thruster allocation matrix $T(\alpha)$ is:

$$T(\alpha) = \begin{bmatrix} c(\alpha_1) & c(\alpha_2) & c(\alpha_3) \\ s(\alpha_1) & s(\alpha_2) & s(\alpha_3) \\ -l_{y1}c(\alpha_1) - l_{x1}s(\alpha_1) & l_{y2}c(\alpha_2) - l_{x2}s(\alpha_2) & l_{x3}s(\alpha_3) \end{bmatrix} \tag{34}$$

Where $c(\alpha_i)$ and $s(\alpha_i)$ stand for $\cos(\alpha_i)$ and $\sin(\alpha_i)$ respectively. So, the A and $B(\alpha)$ matrix are

$$A = \begin{bmatrix} 1 & 0 & 1 & 0 & 1 & 0 \\ 0 & 1 & 0 & 1 & 0 & 1 \\ -l_{y1} & l_{x1} & -l_{y2} & l_{x2} & -l_{y3} & l_{x3} \end{bmatrix} \tag{35}$$

$$B(\alpha) = \begin{bmatrix} c(\alpha_1) & 0 & 0 \\ s(\alpha_1) & 0 & 0 \\ 0 & c(\alpha_2) & 0 \\ 0 & s(\alpha_2) & 0 \\ 0 & 0 & c(\alpha_3) \\ 0 & 0 & s(\alpha_3) \end{bmatrix} \tag{36}$$

Thruster dynamics are described by the following parameters: time constants for the LP-filter are $T_i = 10s$, the cut-off frequencies are $\omega_{n,i} = 0.63$, for $i = 1, .., 3$ and the damping ratio is $\zeta_i = 1$ for $i \in 1, 2, 3$.

The performance index is considered for a quantitative comparison between results of various simulations. The performance index used here is the Integral of Squared Error *ISE*. For the DP system index depend on the error between position and orientation references and position and orientation measured by sensors, namely $e(t) = \eta_{des}(t) - \eta(t)$. The index expression is $ISE = \frac{1}{t_f - t_0} \int_{t_0}^{t_f} e(t)^2 dt$.

In the following we show the comparison between the proposed control system and a conventional PID controller, using a configuration similar to the one reported in [8] for the Cybership I, considering the following case scenarios:

Case 1 The scale model is sailing in calm water with slight disturbances from wind and currents in a short straight movement.

Case 2 The scale model is sailing in slight water with moderate disturbances from wind and currents in a short straight movement.

Case 3 The scale model is sailing in calm water with slight disturbances from wind and currents, desired position and changes 2 times.

Reference positions in the $\{n\}$ frame are shown in Table I. Environmental conditions during tests, in terms of significant wave height H_s, modal frequency w_0, wind velocity V_w and current speed V_c, are shown in Table II. Results in term of ISE performance index are in Table III. The vessel is sailing in quartering sea. This affects the index for the n direction, which is therefore considerably bigger compared to e for all the case scenarios. Results from CASE 1 simulations are shown in Fig. 3. Results from the CASE 3 simulations are shown in Fig. 4. Azimuth thruster angle and torques set by the control allocation algorithms are also show in Fig. 5.

Simulation results show that the DTVS controller guarantees a satisfactory smoother performance with respect to the PID controller in every case considered. The DTVSC can eventually require larger control efforts and could be more complex to deploy and computationally expensive with respect to the PID controller, it guarantees better performance. Results of the CASE 1 simulations, depicted in Fig. 3(b), show that using the PID controller the ship orientation slowly converge to the reference orientation, while the DTVSC controller rapidly brings the system state nearby the sliding surfaces, while the integral action counteract the 2-nd order slowly varying drift forces. While Case 3 simulation results

TABLE III

ISE PERFORMANCE INDEX

	n (surge position)		e (sway position)		ψ (yaw rotation)	
	DTVSC	PID	DTVSC	PID	DTVSC	PID
Case 1	0.0023	0.03	$7.47 \cdot 10^{-6}$	$7.99 \cdot 10^{-6}$	$1.51 \cdot 10^{-5}$	$1.61 \cdot 10^{-5}$
Case 2	0.0073	0.07	$2.1 \cdot 10^{-5}$	$2.13 \cdot 10^{-5}$	$3.64 \cdot 10^{-5}$	$3.98 \cdot 10^{-5}$
Case 3	0.0057	0.024	$5.2 \cdot 10^{-6}$	$5.88 \cdot 10^{-6}$	$1.51 \cdot 10^{-5}$	$1.62 \cdot 10^{-5}$

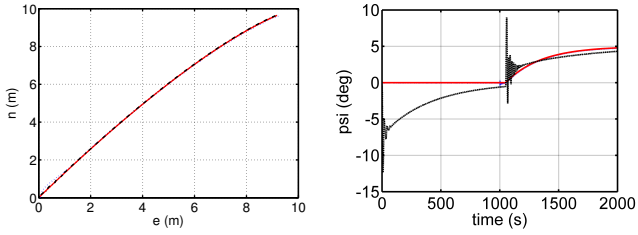

(a) References and simulated path (b) Reference and simulated yaw rotation angle

Fig. 3. CASE 1 - References (red line) and simulated n, e and ψ using DTVS controller (blue and dotted line) and PID (black and dash-dotted line)

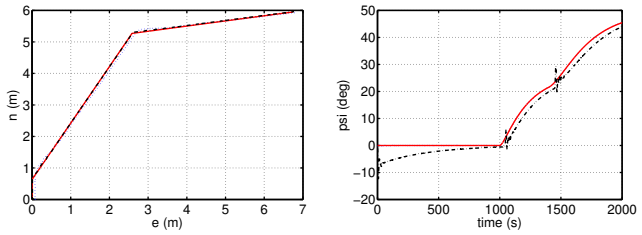

(a) References and simulated path (b) Reference and simulated yaw rotation angle

Fig. 4. CASE 3 - References (red line) and simulated n, e and ψ using DTVS controller (blue and dotted line) and PID (black and dash-dotted line)

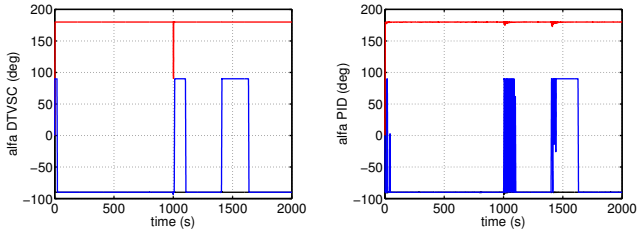

(a) Azimuth angle α using DTVS controller (b) Azimuth angle α using PID

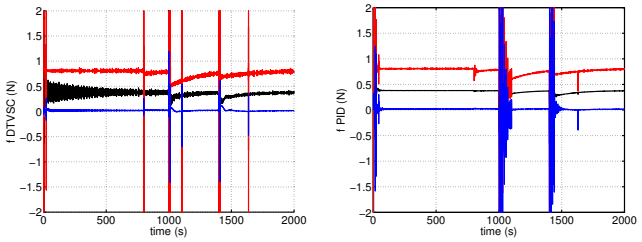

(c) Thruster torque f using DTVSC (d) Thruster torque f using PID

Fig. 5. CASE 3 - First (blue line), second (red line) and third (black line) azimuth thruster's angle α and thrust force f

in Fig. 4(b) show that DTVS control system performs better during reference position changes, notably for the yaw rotation angle. Fig. 5(c) and Fig. 5(d) shows that the price to pay for the performance improvement of the DTVSC is the control effort, while Fig. 5(a) and Fig. 5(b) show how the DLS method implemented for the allocation algorithm helps in preventing further increases of the control efforts, when the azimuth thrusters configuration is near a singular value. Results in Table III show that the worse environmental conditions of CASE 2 respect to CASE 1 are reflected by far larger ISE performance indices both for PID and DTVS controller. Anyway the latter always show better perfomances in terms of ISE index compared to the PID.

VI. Conclusions

The problem of dynamic positioning plays a key role in all those cases where it is not possible to anchor the ship at the seabed, or where the ship's position is bound to a specific point on the bottom. In this paper an architecture is identified for the autonomous dynamic positioning of marine vessel equipped with azimuth thruster using a non-linear discrete control and robust control allocation technique for the resolution of the DP problem. Here we assume state feedback, an extension to output feedback using state observers will be a next step. From a control perspective, it was shown that the DTVS controller satisfy the sliding mode existence condition in a sector depending on the maximum uncertainties of the system. Simulations confirm the robustness of the control scheme in presence of environmental disturbances also in moderate seas and show that DTVSC outperformed classic PID controller.

References

[1] A. J. Sørensen, "A survey of dynamic positioning control systems," *Annual Reviews in Control*, vol. 35, no. 1, pp. 123 – 136, 2011.

[2] J. G. Balchen, N. A. Jenssen, E. Mathisen, and S. Sælid, "A dynamic positioning system based on kalman filtering and optimal control," *Modeling, Identification and Control*, vol. 1, no. 3, pp. 135–163, 1980.

[3] M. J. Grimble, R. J. Patton, and D. A. Wise, "The design of dynamic ship positioning control systems using stochastic optimal control theory," *Optimal Control Applications and Methods*, vol. 1, no. 2, pp. 167–202, 1980.

[4] S. Fang, B. J. Leira, and M. Blanke, "Reliability-based dynamic positioning of floating vessels with riser and mooring system," in *International Conference on Computational Methods in Marine Engineering (MARINE)*, Lisbon, Portugal, Sept. 2011.

[5] E. A. Tannuri and A. C. Agostinho, "Higher order sliding mode control applied to dynamic positioning systems," in *Proc. of the 8th IFAC Conference on Control Applications in Marine Systems*, Rostock-Warnemünde, Germany, sep 2010, pp. 132–137.

[6] I. Lindfors, "Thruster allocation method for dynamic positioning system," Ottawa, Canada, 1993, pp. 3.93–3.106.

[7] O. Sørdalen, "Thruster allocation: Singularities and filtering," in *13th IFAC World Congress*, vol. Q, San Francisco, California, 1996, pp. 369–374.

[8] S. P. Berge and T. I. Fossen, "Robust Control Allocation Of Overactuated Ships; Experiments With A Model Ship," in *Proc. of the 4th IFAC Conference on Manoeuvring and Control of Marine Craft*, Brijuni, Croatia, 1997, pp. 166–171.

[9] T. Fossen and T. Johansen, "A Survey of Control Allocation Methods for Ships and Underwater Vehicles," in *14th Mediterranean Conference onControl and Automation*, Ancona, Italy, June 2006, pp. 1–6.

[10] T. I. Fossen, *Handbook of Marine Craft Hydrodynamics and Motion Control*. Chichester, UK: John Wiley & Sons, Ltd, Apr. 2011.

[11] R. Isherwood, "Wind Resistance of Merchant Ships," *Trans. Inst. Naval Arch., RINA*, vol. 115, pp. 327–338, 1972.

[12] A. Sørensen, S. Sagatun, and T. Fossen, "Design of a dynamic positioning system using model-based control," *Control Engineering Practice*, vol. 4, no. 3, pp. 359 – 368, 1996.

[13] V. Utkin, *Sliding modes in control and optimization*. Berlin Allemagne: Springer-Verlag, 1992.

[14] J. J. Slotine and S. S. Sastry, "Tracking control of non-linear systems using sliding surfaces with application to robot manipulators," in *American Control Conference*, 1983, pp. 132–135.

[15] M. Corradini and G. Orlando, "A discrete adaptive variable-structure controller for mimo systems, and its application to an underwater rov," *IEEE Transactions on Control Systems Technology*, vol. 5, no. 3, pp. 349 –359, may 1997.

[16] F. Benetazzo, G. Ippoliti, S. Longhi, and P. Raspa, "Discrete Time Variable Structure Control for the Dynamic Positioning of an Offshore Supply Vessel," in *Preprints of the 2012 IFAC Workshop on Automatic Control in Offshore Oil and Gas Production*, 2012.

[17] C. Y. Chan, "Discrete adaptive sliding-mode tracking controller," *Automatica*, vol. 33, pp. 999–1002, May 1997.

[18] H. A. Barker, "Discrete-Time Signals and Systems," *Electronics And Power*, vol. 30, no. 2, p. 159, 1984.

[19] A. B. Mahfouz and H. W. El-Tahan, "On the use of the capability polar plots program for dynamic positioning systems for marine vessels," *Ocean Engineering*, vol. 33, no. 89, pp. 1070 – 1089, 2006.

[20] T. Solvin, "Underactuated dynamic positioning with model test," Master's thesis, Trondheim, Norway, 2011.

[21] T. D. Nguyen, A. J. Sørensen, and S. Tong Quek, "Design of hybrid controller for dynamic positioning from calm to extreme sea conditions," *Automatica*, vol. 43, pp. 768–785, May 2007.